energies

Article

Quantitative Evaluation of Water-Flooded Zone in a Sandstone Reservoir with Complex Porosity–Permeability Relationship Based on J-Function Classification: A Case Study of Kalamkas Oilfield

Xuanran Li [1], Jingcai Wang [1], Dingding Zhao [2,3,*], Jun Ni [1], Yaping Lin [1], Angang Zhang [1], Lun Zhao [1] and Yuming Liu [2,3,*]

1 PetroChina Research Institute of Petroleum Exploration & Development, Beijing 100083, China
2 State Key Laboratory of Petroleum Resources and Prospecting, China University of Petroleum-Beijing, Beijing 102249, China
3 College of Geosciences, China University of Petroleum-Beijing, Beijing 102249, China
* Correspondence: 2019310048@student.cup.edu.cn (D.Z.); liuym@cup.edu.cn (Y.L.)

Citation: Li, X.; Wang, J.; Zhao, D.; Ni, J.; Lin, Y.; Zhang, A.; Zhao, L.; Liu, Y. Quantitative Evaluation of Water-Flooded Zone in a Sandstone Reservoir with Complex Porosity–Permeability Relationship Based on J-Function Classification: A Case Study of Kalamkas Oilfield. *Energies* **2022**, *15*, 7037. https://doi.org/10.3390/en15197037

Academic Editor: Reza Rezaee

Received: 12 August 2022
Accepted: 21 September 2022
Published: 25 September 2022

Abstract: The water-flooded zone in a sandstone reservoir with a complex porosity–permeability relationship is difficult to interpret quantitatively. Taking the P Formation of Kalamkas Oilfield in Kazakhstan as an example, this paper proposed a reservoir classification method that introduces the J-function into the crossplot of resistivity and oil column height to realize the classification of sandstone reservoirs with a complex porosity–permeability relationship. Based on the classification results, the initial resistivity calculation models of classified reservoirs were established. The oil–water seepage experiment was performed for classified reservoirs to measure the lithoelectric parameters and establish the relationship between water production rate and resistivity for these reservoirs, and then water production was quantitatively calculated according to the difference between the inverted initial resistivity and the measured resistivity. The results show that the reservoirs with an unclear porosity–permeability relationship can be classified by applying the J-function corresponding to grouped capillary pressure curves to the crossplot of oil column height and resistivity, according to the group average principle of capillary pressure curves. This method can solve the problem that difficult reservoir classification caused by a weak porosity–permeability correlation. Moreover, based on the results of reservoir classification, the water production rate and resistivity model of classified reservoirs is established. In this way, the accuracy of quantitative interpretation of the water-flooded zone in the reservoir can be greatly improved.

Keywords: complex porosity–permeability relationship; water-flooded zone; oil column height; reservoir classification; capillary pressure; resistivity; water production rate

1. Introduction

Kalamkas Oilfield is a typical high water-cut layered sandstone reservoir, which has been developed for 42 years, in North Ustyurt Basin, Kazakhstan. The water cut has reached 94%, while only 25% of the original oil in place (OOIP) has been recovered. Most wells suffered from water-out, which severely affected the enhanced oil recovery (EOR) [1–3]. The target strata in the Kalamkas Oilfield are characterized by complex lithology (including coarse sandstone, silty-fine sandstone, and argillaceous sandstone) and diverse reservoir fluids, consisting of gas zone, low-resistivity oil zone, normal oil zone, and oil–water zone, as well as water-flooded zone and water zone. The sandstone reservoir is highly heterogeneous, with the porosity and permeability not clearly correlated, making the permeability calculation and reservoir classification very challenging [4]. Currently, most calculations of water cuts in water-flooded zones are less precise, or quantitative classifications of water-flooded zones involve too many procedures in a long period, so they are far behind the field applications [5,6]. Accordingly, a quantitative evaluation of the water-flooding intensity of such high water-cut reservoirs with complex porosity–permeability relationship is fundamental for predicting and recovering the remaining oil in many similar high water-cut sandstone oilfields.

A reasonable reservoir classification is crucial to the evaluation of water-flooded zones in reservoirs with weak porosity–permeability relationships and strong heterogeneity [7–10]. There are mainly three reservoir classification methods [11–15]: (1) porosity and permeability, the key physical properties of reservoirs, are taken as the main parameters to classify the reservoirs as, for instance, high-porosity and high-permeability reservoirs, medium-porosity and medium-permeability reservoirs, and low-porosity and low-permeability reservoirs; (2) porosity and permeability are combined with microscopic parameters (e.g., pore structure) to classify the reservoirs through probability statistics of numerous physical property parameters, which is a multivariate evaluation method [16]; and (3) the concept of flow unit is followed, that is, the identical flow units have similar physical features and flow capacity, generally leading to similar water-flooding and remaining oil distribution characteristics. The first and third methods are essentially rooted in the function of porosity and permeability, but they cannot work well when there is no clear correlation between the two parameters. The second method yields relatively low-accurate results in reservoirs with strong heterogeneity and complex pore structure and requires a vast amount of data that can reflect the pore structure, such as grain size, pore throat radius, and sorting.

In recent years, with the development of computer technology, the combination of well logging curves and artificial intelligence methods has also been widely used to identify water-flooded zones. These methods include: the fuzzy neural network method, general neural network method, hybrid computing neural network method, and integrated classifier method [17–20]. In these methods, the fuzzy neural network needs multiple factors to make a comprehensive judgment, and too many input factors are likely to limit application; the general neural network has low convergence speed, and it is easy to fall into local optimal solution; the hybrid computing neural network method has higher requirements for the original data as a whole. The process neural network introduces the original form of the well logging curve as the sample input, which has improved the recognition efficiency to a certain extent. However, the interpolation fitting will produce fitting errors, resulting in large cumulative errors. Due to some limitations of the above methods, there are still problems of lower recognition accuracy and efficiency [21–23].

With P Formation in Kalamkas Oilfield as an example, based on the knowledge that reservoir resistivity is the comprehensive reflection of pore structure and oil column height, the resistivity vs. oil column height crossplot was established, and the J-function of capillary pressure curves was established and incorporated into the resistivity vs. oil column height crossplot. On this basis, the reservoirs with the complex porosity–permeability relationship were classified. For each class of reservoirs, the initial resistivities under different oil column heights were inverted by using the fitted relationships of multiple parameters; the oil–water flow experiment was performed to determine the oil–water relative permeability, which was then combined with the Archie formula to build the water cut and resistivity model for dividing the water-flooding levels of reservoirs. The initial and current resistivities were compared to fix the decline of resistivity, by which the water-flooding intensity of reservoirs was quantitatively evaluated. This paper proposes a simple method for reservoir classification by using only conventional well logging data. In particular, this method has a good application effect in the reservoirs with the worse porosity–permeability relationship. It requires a large number of capillary pressure test data and is not applicable to the oilfields with few coring data and incomplete capillary pressure tests.

2. Regional Geology

The Middle Jurassic P Formation, the major producing system in Kalamkas Oilfield, is a layered, unsaturated, stratigraphically-unconformable reservoir with a gas cap and edge water. The P Formation pay zones are mainly composed of fine sandstone and siltstone, with a high shale content (20–35%). The core porosity experiments show that the reservoir has a medium-high porosity (avg. 28.6%) and a medium-high permeability (avg. 357.4 mD), and it is a kind of clastic rock reservoir common in Central Asia. The P Formation was initially developed by water injection in 1980. Currently, it is in the stage of development with a high water cut (93%), with 20.4% of geological reserves recovered, and daily oil production of 0.5–55 t, and a water cut of 0–98% for new wells, indicating greatly different water flooding degrees in the reservoir. A large number of core analysis and production data show that the P Formation sandstone reservoir in Kalamkas Oilfield is complex and diverse in pore structure, obviously different in reservoir quality [24,25], and very strong in heterogeneity. The core grain size analysis reveals (Figure 1) that the reservoir rocks contain a generally high content of fine particles, of which, 37.4% exhibit the components with grain size less than 0.01 mm, and which are mainly clay mineral particles, except for a small part of fine silts. According to the porosity–permeability relationship, the lithology and pore structure are complex, and the correlation between porosity and permeability is very weak (Figure 2). After long-term water flooding, fine particles, such as clay minerals, block the port throats, thereby aggravating the reservoir heterogeneity, so the water flooding law is very complex [26,27]. With the further development, the quantitative research on water-flooded zone is particularly important.

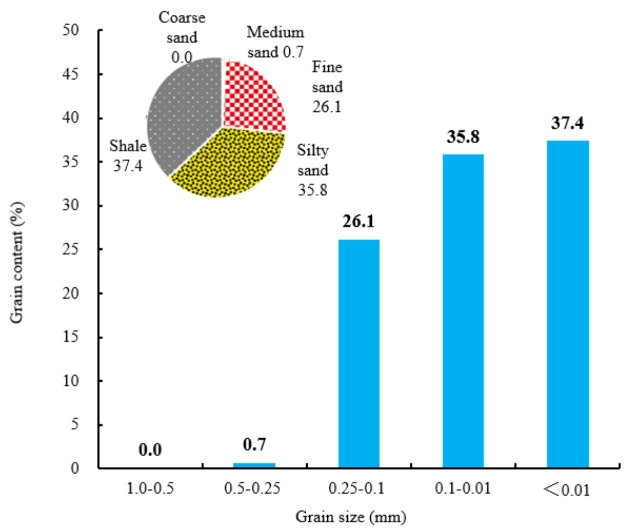

Figure 1. Grain size analysis of P Formation in Kalamkas Oilfield.

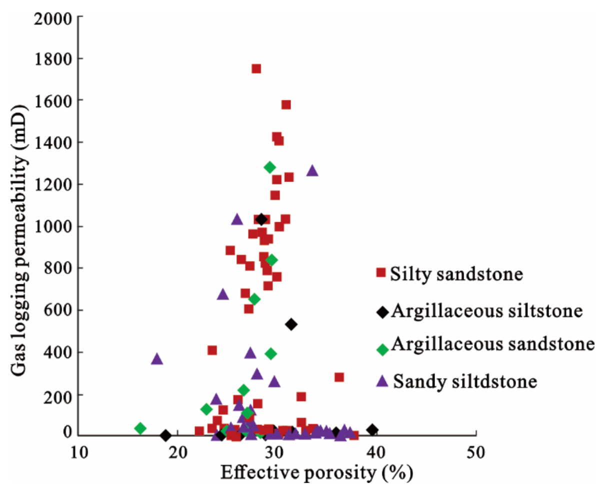

Figure 2. Porosity–permeability relationship of P Formation in Kalamkas Oilfield.

3. Research Method and Data Source

3.1. Research Method

The research is completed in five steps (Figure 3).

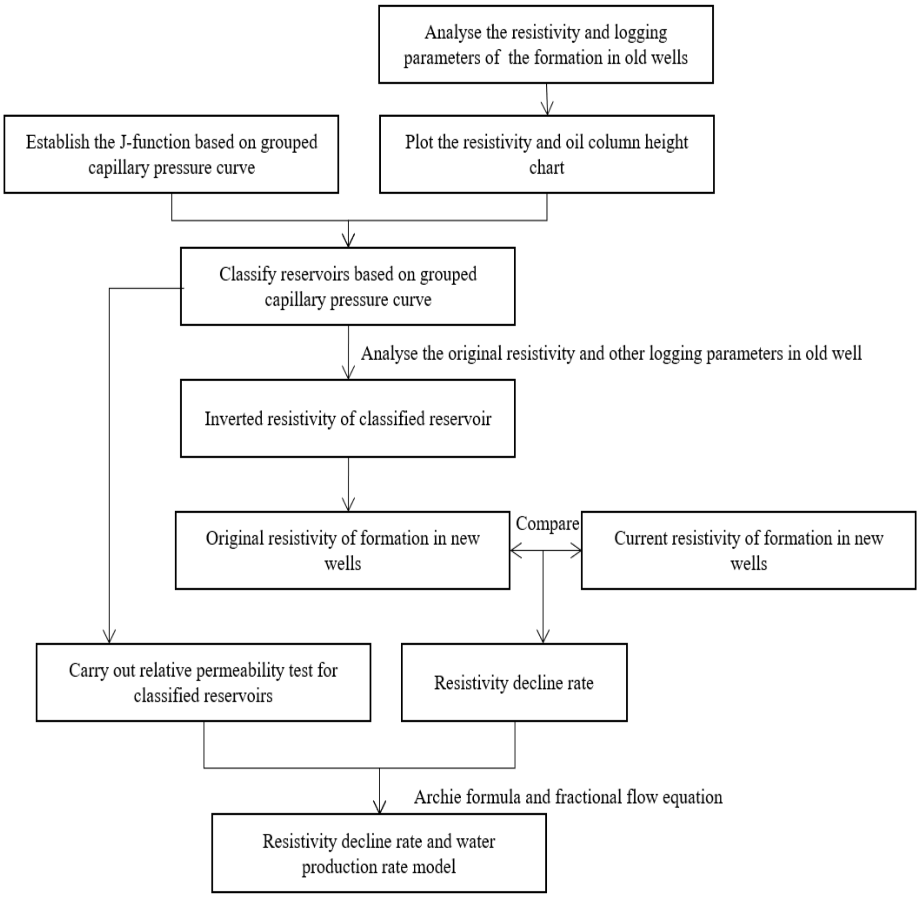

Figure 3. The quantitative evaluation process of the water-flooded zone in sandstone reservoir with complex porosity–permeability relationship.

Step 1: Group the capillary pressure curves and calculate the average value of each group (J-function). Capillary pressure curves were obtained on a CPPP-300 group capillarimeter using the semi-permeable membrane method.

Step 2: Collect the logging data and oil test data of existing old wells, and establish the crossplot of oil column height and resistivity; incorporate the grouped capillary pressure curves to the crossplot, and classify the reservoirs with the complex porosity–permeability relationship.

Step 3: Collect the conventional logging data of existing old wells, analyze the laws of initial reservoir resistivity, oil column height, and natural gamma, and establish the expression of the relation between initial reservoir resistivity, oil column height, and natural gamma by using multiple regression methods.

Step 4: Obtain the initial resistivity of each reservoir by using the relational expression in the above step for newly drilled production wells, and determine the resistivity decline rate from the current resistivity obtained from new well logging and the calculated initial resistivity.

Step 5: Perform a relative permeability test for each class of reservoirs, and establish the water cut and resistivity decline rate model of classified reservoirs by using the Archie formula and fractional flow equation, to accurately predict the water-flooding degree of each reservoir of the new well.

3.2. Data Source

This study used the capillary pressure test data of 33 samples of P Formation in Kalamkas Oilfield (Table 1). It is found that the irreducible water saturation is 11–41%, the saturated median pressure is 0.02–0.35 MPa, the gas logging porosity is 21–37%, and the gas logging permeability is (1.88–1140) $\times 10^{-3}$ μm^2. The grain size analysis was made on 161 samples from 10 coring wells, basically covering all target horizons, with a grain density of 2.47–2.96 g/cm^3 and a rock density of 1.67–2.19 g/cm^3 (Table 2). The reservoir classification was completed with a logging interpretation data of 502 wells and a resistivity of 2.3–40 ohm (avg. 6.52 ohm). It was determined that the porosity is 23–38% (avg. 27.5%), the permeability is 4.8–3520 mD (avg. 425 mD), and the shale content is 3–45% (avg. 18%) (Table 3).

Table 1. Capillary pressure test data of P Formation core samples.

Core No.	Core Length/cm	Core Diameter/cm	Porosity (Water)/%	Porosity (Gas)/%	Gas Logging Permeability/ 10^{-3} μm^2	RQI	Saturated Median Pressure/Mpa	Minimum Wet Phase Saturation (Irreducible Water Saturation)/%
486	5.3	3.8	25.6	25.7	18.4	8.5	0.1	25.0
488	5.4	3.4	25.1	25.1	1.9	2.7	0.1	33.0
489	5.2	3.7	21.0	21.1	2.7	3.6	0.4	41.0
491	5.5	3.8	22.8	22.9	5.3	4.8	0.3	11.0
495	5.2	3.5	26.6	26.8	15.0	7.5	0.2	30.0
41	5.2	3.8	25.9	25.9	12.3	6.9	0.2	37.0
496	5.0	3.5	29.7	29.7	51.6	13.2	0.2	25.0
497	5.1	3.8	30.7	30.8	53.6	13.2	0.2	24.0
492	5.2	3.6	29.7	29.8	81.4	16.5	0.2	26.0
493	5.5	3.1	30.1	30.2	60.4	14.2	0.2	26.0
494	5.5	3.3	29.8	30.1	58.5	13.9	0.1	22.0
487	5.2	3.5	29.5	29.6	36.8	11.2	0.1	26.0
503	5.2	3.8	33.6	33.8	533.8	39.7	0.1	21.0
513	4.9	3.5	32.9	33.2	475.4	37.9	0.2	22.0
514	5.2	3.2	32.1	32.1	404.7	35.5	0.1	21.0
515	5.3	3.4	32.0	32.1	309.7	31.1	0.1	20.0
516	5.5	3.5	32.3	32.4	482.2	38.6	0.1	21.0
517	5.6	3.5	30.8	30.8	345.2	33.5	0.2	24.0
527	5.3	3.8	33.0	33.1	448.4	36.8	0.1	21.0
528	5.3	3.8	32.6	32.7	414.6	35.6	0.1	20.0
518	5.2	3.8	32.2	32.2	1020.0	56.3	0.2	21.0
519	5.2	3.8	34.1	34.2	845.4	49.7	0.1	17.0
520	5.4	3.7	30.6	30.7	1140.0	60.9	0.1	18.0
521	5.0	3.8	30.8	30.8	721.5	48.4	0.2	23.0
522	5.3	3.8	32.2	32.3	1120.0	58.9	0.1	18.0
523	5.2	3.7	30.9	31.0	758.5	49.5	0.1	21.0
524	5.1	3.5	32.6	32.7	1070.0	57.2	0.1	16.0
525	4.8	3.2	33.5	33.5	880.9	51.3	0.1	18.0
526	5.3	3.1	31.0	31.1	951.4	55.3	0.1	19.0
3	5.2	3.6	36.9	36.9	821.9	47.2	0.0	18.0
6	5.7	3.2	30.8	30.8	394.7	35.8	0.0	22.0
23	4.9	3.1	35.1	35.1	654.9	43.2	0.2	19.0
28	5.7	3.3	35.8	35.8	522.4	38.2	0.2	19.0

Table 2. Grain size analysis results of P Formation.

Formation	>1	1.0–0.5	0.5–0.25	0.25–0.1	0.1–0.01	<0.01
		Coarse sand	Medium sand	Fine sand	Silty sand	Mud
P	0.00	0.01	0.66	26.13	35.81	37.38

Table 3. Partial logging interpretation data of 502 wells in the P Formation.

Well Name	Well Type	Start Depth (m)	End Depth (m)	GZ3 Average	Oil Column Height	GR Relative Value	Inverted Resistivity	Class of Reservoir	GR	VSH (V/V)	SW (V/V)	PERM
XX84	Production well	732.8	738.8	9.0	111.5	83.8	5.4	III	155.0	0.1	0.3	328.0
XX57	Production well	742.1	744.6	7.6	104.4	81.3	5.2	III	130.0	0.1	0.4	444.5
XX24	Production well	754.5	757.3	6.9	92.9	82.4	4.8	III	136.0	0.2	0.1	310.5
XX67	Production well	740.9	745.8	6.8	103.3	80.0	5.2	III	124.0	0.2	0.3	160.3
XX72	Production well	745.3	747.1	6.2	101.8	85.7	5.0	III	150.0	0.2	0.3	11.6
XX63	Production well	744.3	749.1	19.5	101.2	73.8	11.4	II	104.0	0.1	0.2	283.9
XX73	Production well	740.4	748.4	18.3	101.6	81.5	10.6	II	106.0	0.1	0.2	138.9
XX46	Water injection well	745.7	751.4	15.6	97.5	80.0	10.4	II	124.0	0.2	0.2	301.9
XX39	Production well	760.3	764.8	15.5	83.9	77.9	9.6	II	113.0	0.2	0.2	290.9
XX15	Production well	763.9	767.7	14.6	82.4	80.6	9.1	II	141.0	0.2	0.2	167.5
XX54	Production well	807.4	811.0	28.3	37.6	81.5	12.2	I	137.0	0.1	0.1	1537.5
XX72	Water injection well	773.3	782.2	27.9	68.2	76.5	17.9	I	146.8	0.2	0.2	229.3
XX21	Production well	812.6	814.5	27.1	36.4	70.3	14.8	I	116.0	0.1	0.2	206.8
XX54	Production well	774.5	784.6	26.3	65.4	81.2	16.3	I	134.0	0.1	0.1	317.2
XX76	Production well	747.7	758.2	24.6	88.9	90.0	17.6	I	162.0	0.1	0.1	482.5

4. Result

4.1. Logging Responses of Water-Flooded Zone

After long-term water injection development, the water cut of the sandstone reservoir increases continuously. After entering the reservoir, the injected water interacts with the reservoir, changing the fluid properties, pore structure, rock physicochemical properties, and oil–water distribution of the reservoir to a certain extent. This change will cause the variation of logging curves. Determining the logging responses is fundamental for locating the water-flooded point and confirming the water-flooding degree [28–30].

4.1.1. Resistivity Logging

Resistivity is an important parameter reflecting the fluid properties of the reservoir. The P Formation has been developed for 41 years by reinjecting the waste water. The salinity of injected water is close to the initial salinity of the formation, being about 105,000–150,000 mg/L. The water saturation during water flooding is a gradual process, which can be roughly divided into the early stage with low water cut, the middle stage with medium water cut, and the late stage with high water cut. In the early stage with low water cut, injected water displaces the movable oil in the reservoir and exchanges ions with the initial formation water in the swept zone. Since the P Formation reservoir is developed by waste water reinjection, and the initial formation water is close to the injected water in salinity, the reservoir fluid can reach dynamic balance very quickly, and the reservoir resistivity decreases with the increase in water saturation Sw. At this time, there is no water at the outlet end. With the progress of development, the oilfield enters the middle stage with a medium water cut, resulting in a water breakthrough at the outlet end. The injected water continues to drive out the movable oil and further mixes with the liquid mixture in the swept zone. In this process, the resistivity of the liquid mixture changes greatly. In the late stage with high water cut, the reservoir is completely flooded, the injected water can only drive out a small amount of oil, and the resistivity of the liquid mixture almost reaches the resistivity of the injected water [28,29]. The resistivity generally decreases with the increase in water saturation. The resistivity of the water-flooded zone in the P Formation shows an obvious downward trend. When water flooding is serious, the resistivity of the water-flooded zone is very close to that of the water zone (Figure 4).

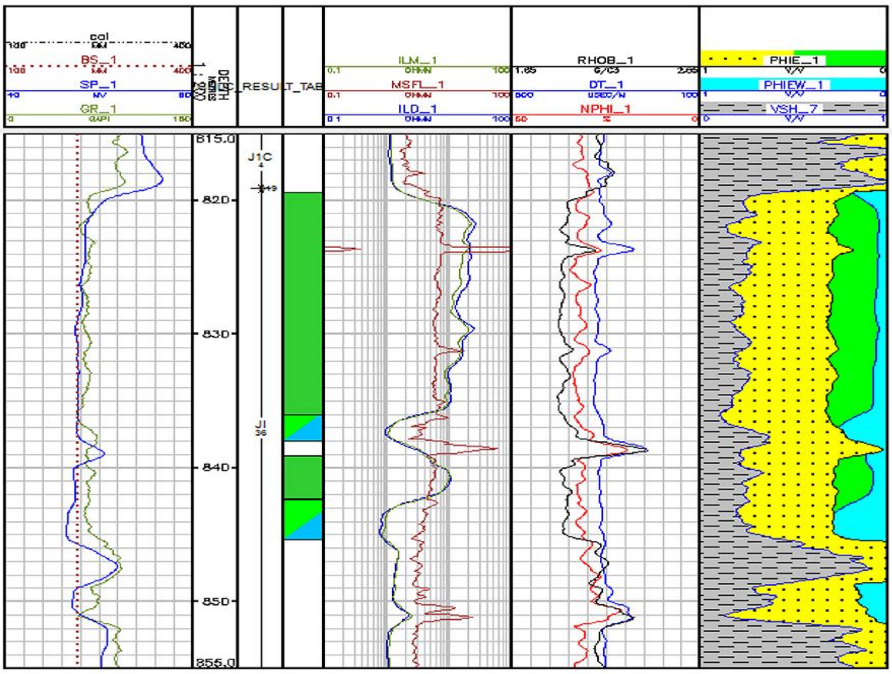

Figure 4. Interpretation of water-flooded zone of Well xx36 in P Formation.

4.1.2. Spontaneous Potential Logging

The spontaneous potential (SP) logging response was analyzed to locate the water-flooded point in the reservoir. According to the previous study [24], in the interpretation of water-flooded zones in the sandstone reservoir, the comprehensive influence of injected water and oil saturation on SP can be expressed by Formula (1) below. Since the salinity of the injected water in the P Formation is close to that of the initial formation water, the baseline shift of SP and the amplitude change of SP are not obvious after water flooding of some reservoirs (Figure 4).

$$SP = -K_C \times \log \frac{R_{mf}}{R_w} + K \times \log \frac{R'_w}{R_w} = -K_C \times \log \frac{R_{mf}}{R_w} - K \times \log S_w \tag{1}$$

where the first term represents the influence of injected water on spontaneous potential (SP), and the second term represents the influence of oil saturation on SP. The change of SP log in water flooding results from the stacking of these two processes.

4.2. Classification of Sandstone Reservoirs with a Complex Porosity–Permeability Relationship Based on Average Capillary Pressure (J-Function)

When logging data are used to identify water-flooded zones, reservoir classification is an effective way to improve the identification accuracy of water-flooded zones in heterogeneous reservoirs. Reasonable reservoir classification is particularly critical in the interpretation of water-flooded zones in reservoirs with no obvious porosity–permeability relationship. Many scholars classify reservoirs according to the principle that the same flow units have similar physical properties and flow capacity. Wang et al. [14] classified the reservoirs with permeability as the primary parameter and porosity as the second parameter. Yang et al. [10] proposed a multivariate evaluation method combining porosity and permeability with microscopic parameters. Gunter et al. [13] classified the reservoirs according to the concept of flow unit. Essentially, these methods are based on the function of porosity and permeability, but are limited for reservoirs with a very unclear porosity–permeability relationship. According to the conventional core analysis, capillary pressure curve shape, logging responses, and analysis of logging facies and lithofacies, the capillary pressure curves of Kalamkas Oilfield are divided into three groups (Figure 5): Type 1, Type 2, and Type 3. Type 1 capillary pressure curves are the longest in the middle gentle segment and the lowest in position, and represent the reservoirs with the best sorting and the largest throat radius, being the reservoirs with the best physical properties. Type 2 capillary pressure curves have a slightly shorter middle gentle segment and higher position than Type 1, and represent the reservoirs with moderate physical properties. Type 3 capillary pressure curves have the shortest and highest gentle segment, and represent the reservoirs with the worst physical properties. Accordingly, the average value of each group of capillary pressure curves (J-function) was obtained. Figure 6 shows the J-function of the P Formation in Kalamkas Oilfield. It can be seen that the data points are concentrated, indicating that the grouping of capillary pressure curves is reasonable.

Oil column height, porosity, pore connectivity, and oil–water density difference are the main factors affecting the initial resistivity of the reservoir. The higher the oil column height, the better the pore structure, the stronger the hydrocarbon charging capacity, and the higher the resistivity [30–33]. Accordingly, the crossplot of resistivity and oil column height can be established to characterize the pore structure and reflects the physical properties gradually deteriorating from the data point to the right. According to the Archie formula [33], there is a direct relationship between reservoir resistivity and water saturation. According to the concept of capillary force, the capillary pressure is directly proportional to the rising height of the wetting phase in the capillary. Therefore, the height of the oil column in the reservoir is a direct reflection of the value of capillary pressure. According to the above principle, the crossplot of resistivity and oil column height can be combined with the capillary pressure curves. According to the capillary pressure measured in the laboratory test of cores, the J-function (average capillary pressure) of three classes of reservoirs (good, moderate, and poor) was established, as shown in Figures 5 and 6. Based on the J-function of existing coring wells, the continuous capillary pressure curves can be reconstructed for the non-coring intervals [34,35]. The reconstructed multiple capillary pressure curves are applied to the crossplot. The reservoirs of the P Formation can be classified as I, II, and III (Figure 7), corresponding, respectively, to good, moderate, and poor porosity and permeability, which are arranged in turn from left to right on the crossplot. This classification can eliminate the influences of permeability and porosity and realize the classification of highly heterogeneous reservoirs with no obvious porosity–permeability relationship.

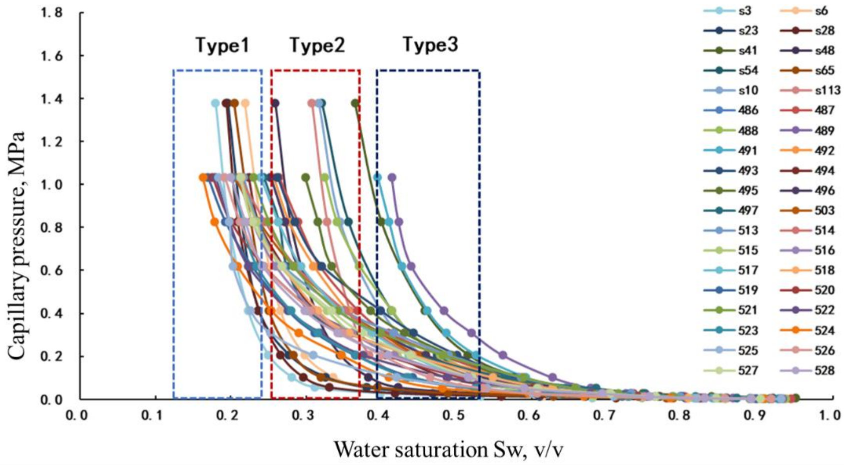

Figure 5. Grouping of capillary pressure curves.

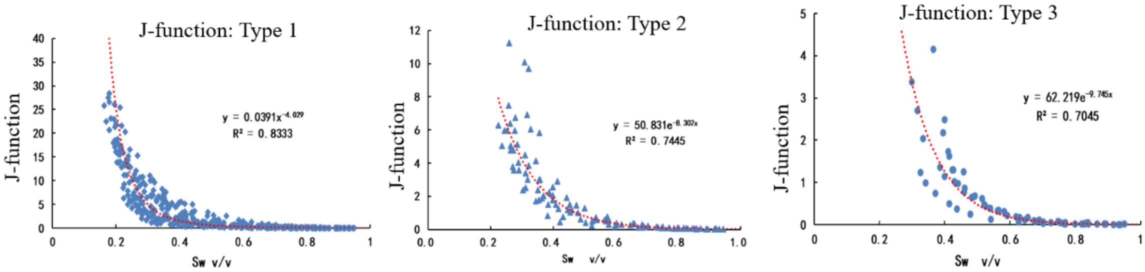

Figure 6. J-functions of grouped capillary pressure curves.

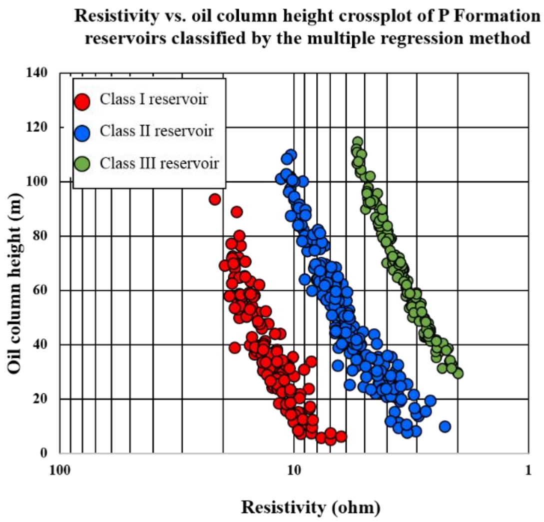

Figure 7. Crossplots of resistivity and oil column height of P Formation reservoirs.

According to the analysis of logging interpretation results of Classes I, II, and III reservoirs (Table 4), Class I reservoirs, with the porosity of more than 28% and the relative GR value of less than 76%, are mainly composed of fine sandstone, with a small amount of medium and coarse sandstone, and contain the sedimentary facies dominated by underwater distributary channel of delta front; Class II reservoirs, with the porosity of 22–28% and the relative GR value of 76–85%, are mainly composed of siltstone, and contain both distributary channel and estuarine bar; and Class III reservoirs, with the porosity of less than 22% and the relative GR value of greater than 85%, are mainly composed of argillaceous sandstone, and contain a distal bar and bar margin deposits.

Table 4. Logging interpretation results of reservoirs.

Class of Reservoirs	Porosity (%)	Permeability (mD)	Relative GR Value (%)	Shale Content (%)	Lithology
I	>28	>600	<76	<21	Mainly sandstone and fine sandstone
II	22~28	30~600	76~85	21~32	Mainly siltstone
III	<22	<30	>85	>32	Mainly argillaceous sandstone

4.3. Initial Resistivity Inversion and Water Production Rate Calculation

The resistivity is sensitive to the water flooding degree. The change of resistivity is the main parameter to identify the water-flooded zones. The water-flooded zones exhibit the decline of resistivity to different degrees, while the non-flooded zones basically do not have a change in resistivity. Therefore, the water-flooded zone can be identified according to the difference between the initial resistivity and the current resistivity.

4.3.1. Initial Resistivity Inversion of Classified Reservoirs

Archie [33] discussed the relationship between resistivity, water saturation, and porosity under the condition that the rock skeleton is not conducive. Generally, the larger the porosity and the better the pore connectivity, the stronger the oil charging capacity. When the oil saturation and formation water resistivity are higher, the resistivity of the reservoir is higher and the oil column height is larger. When the oil saturation and formation water resistivity are lower, the resistivity of the reservoir is lower and the oil column height is smaller. Through the analysis of the correlation between resistivity, oil column height, relative GR value, and shale content of P Formation reservoirs in old wells, it is found that the correlation between relative GR value, oil column height, and resistivity of the reservoir is good (Figure 8), which shows that oil column height and pore structure are the key parameters to control reservoir resistivity. For the classified reservoirs, the initial resistivity was calculated by multiple regression of oil column height and shale content. Based on the data of 141 old wells (these representative data basically cover all target horizons both vertically and horizontally), multiple regression was conducted for the classified reservoirs with the formulas as follows:

$$\text{Class I: reservoirs: Ri} = 26.6858 + \text{H} \times 0.145736 - \text{DGR} \times 0.2447 \tag{2}$$

$$\text{Class II: reservoirs: Ri} = 11.75654 + \text{H} \times 0.078969 - \text{DGR} \times 0.11312 \tag{3}$$

$$\text{Class III: reservoirs: Ri} = 3.53265 + \text{H} \times 0.039465 - \text{DGR} \times 0.02916 \tag{4}$$

$$\text{DGR} = 100 \times (\text{GR}/\text{GR}_{max}) \tag{5}$$

where Ri is the inverted initial resistivity of the reservoir, ohm; H is the oil column height, m; DGR is the relative GR value, %; GR is the measured natural gamma value, API; and GR_{max} is the value of mudstone marker layer.

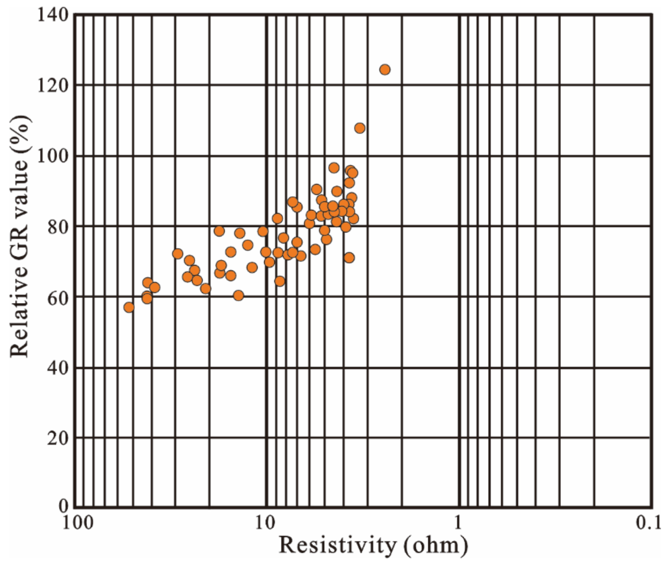

Figure 8. Crossplots of resistivity and relative GR value of P Formation reservoirs.

4.3.2. Calculation of Water Production Rate of Water-Flooded Zone

Relative permeability is one of the basic parameters for analyzing the multiphase flow in a reservoir. The water production rate can be calculated directly by using the relative permeability [32]. The oil–water relative permeability ratio in the relative permeability curve is relative to the water saturation. The relationship between resistivity and water saturation can be obtained through the Archie formula. Thus, the relationship between resistivity and water production rate can be established. In particular, m, n, a, and b in the Archie formula are determined from core litho-electric experiment and R_w from water analysis data statistics. In this study, a = 1.1, b = 1, m = 1.77, n = 1.9, formation water resistivity R_w = 0.05 ohm.

$$F_w = Q_w/(Q_0 + Q_w) = 1/\left(1 + B \times \frac{k_{ro}}{k_{r_w}} \times \frac{\mu_w}{\mu_o}\right) \tag{6}$$

where K_{ro} is the oil relative permeability, 10^{-3} μm^2; K_{rw} is the water relative permeability, 10^{-3} μm^2; and μ_w/μ_o is the viscosity ratio of water to oil.

$$S_w = \left[\frac{abR_w}{R_t\Phi^m}\right]^{\frac{1}{n}} \tag{7}$$

where R_t is the resistivity of undisturbed formation, Ω·m; S_w is water saturation, decimal; a, b, m, and n are lithology coefficient, cementation index, and saturation index in litho-electric parameters, respectively; Φ is the effective porosity, decimal; and R_w is the formation water resistivity, Ω·m.

As classified, the reservoirs with the porosity ∅ < 23 are Class III reservoirs, the reservoir with the porosity of 23 < ∅ < 27 is a Class II reservoir, and the reservoir with the porosity ∅ > 27 is a Class I reservoir. The relative permeability test was carried out for each class of reservoirs (Figure 9). In Figure 9a, the oil–water two-phase flow area is wide, the endpoint permeability is high, and the irreducible water saturation is low, indicative of reservoirs with large and well-connected pores. In Figure 9b, the oil–water two-phase flow area is narrower, the endpoint permeability is lower, and the irreducible water saturation is higher than that in Figure 9a, indicative of reservoirs with relatively poor physical properties, and small but moderately-connected pores. In Figure 9c, the oil–water two-phase flow area is narrow and the endpoint permeability is low, indicative of sandstone reservoirs with high shale content and poor connectivity. According to the Specification for Logging Data Processing and Interpreting of Water-flooded Zone (SY/T 6178-2017) [31], the water cut of the water-flooded zone can be divided into: $f_w \leq 10\%$ (clastic rocks), $10\% < f_w \leq 40\%$ (low level), $40\% < f_w \leq 80\%$ (moderate level), $80\% < f_w < 90\%$ (high level), and $f_w \geq 90\%$ (ultra-high level); accordingly, by the water-flooding intensity, each class of reservoir can be divided into non-water-flooded (oil zone), weakly water-flooded, moderately water-flooded, and highly water-flooded. Based on the relative permeability test, the relationship between water cut and water saturation is established for each class of reservoirs, and the relationship between water saturation and resistivity (or resistivity decline rate or RDR) under the experimental conditions is calculated from the Archie formula. Therefore, the relational expression between water cut and RDR for each class of reservoirs can be obtained (Figure 10a–c), and then the quantitative evaluation model of water-flooded zones can be built. According to Formulas (2)–(5), the initial resistivity can be determined from the basic logging parameters. Then, the difference between the initial resistivity and the measured resistivity after water flooding is obtained, and the difference (i.e., RDR) is brought into the relational expression between RDR and water cut (Figure 10), so as to realize the quantitative evaluation of water-flooded zones. In Class I reservoirs, those with RDR > 80% are extremely highly water-flooded zones, those with 69% < RDR < 80% are highly water-flooded zones, those with 41% < RDR < 60% are moderately water-flooded zones, and those with RDR < 41% are weakly water-flooded or oil zones. In Class II reservoirs, those with RDR > 68% are extremely highly water-flooded zones, those with 62% < RDR < 68% are highly water-flooded zones, those with 43% < RDR < 62% are moderately water-flooded zones, and those with RDR < 43% are weakly water-flooded or oil zones. In Class III reservoirs, those with RDR > 57% are extremely highly water-flooded zones, those with 49% < RDR < 57% are highly water-flooded zones, those with 37% < RDR < 49% are moderately water-flooded zones, and those with RDR < 37% are weakly water-flooded or oil zones.

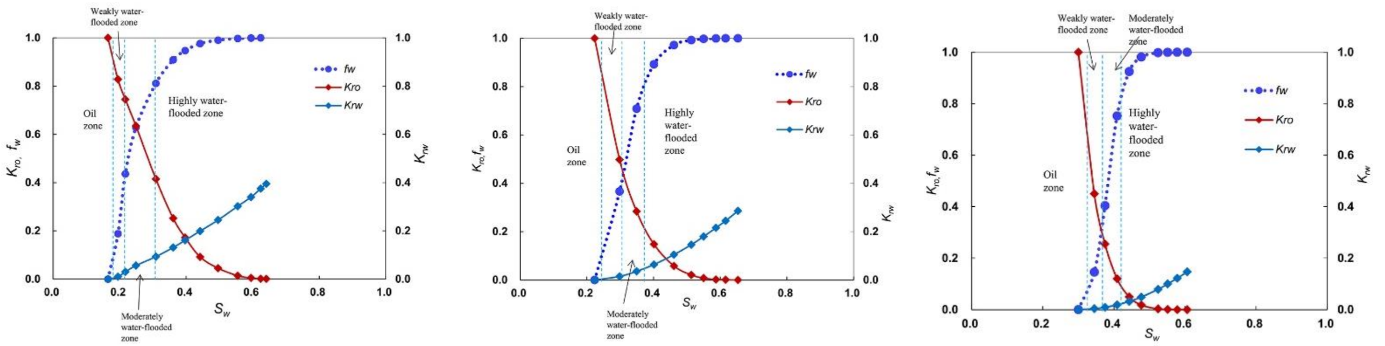

(**a**) (**b**) (**c**)

Figure 9. Oil–water relative permeability of classified reservoirs. (**a**) Class I reservoirs, (**b**) Class II reservoirs, and (**c**) Class III reservoirs.

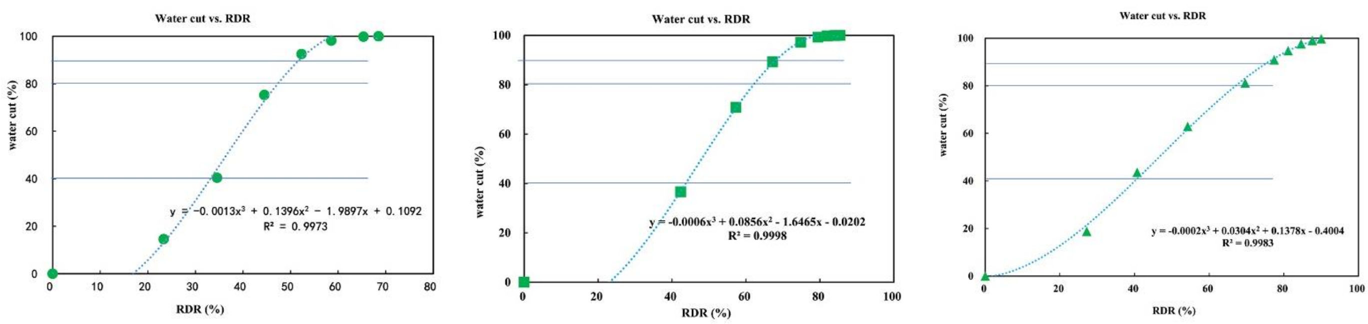

(**a**) (**b**) (**c**)

Figure 10. Relationship between resistivity decline rate (RDR) and water production rate of classified reservoirs. (**a**) Class I reservoirs, (**b**) Class II reservoirs, and (**c**) Class III reservoirs.

According to the above classification criteria and the latest model established, water-flooded zones in 177 reservoirs of 37 new wells in the P Formation of Kalamkas Oilfield were identified. It is found that Class I reservoirs account for about 54%, Class II reservoirs account for about 39%, and Class III reservoirs account for about 7%. The remaining oil in the P Formation is mainly distributed in relatively poor Class III and Class II reservoirs (Table 5).

Table 5. Water-flooded zones in classified reservoirs in P Formation, Kalamkas Oilfield.

Class of Reservoirs	Proportion	Highly Water-Flooded	Moderately Water-Flooded	Weakly Water-Flooded	Non-Water-Flooded
I	54%	60%	23%	7%	9%
II	39%	25%	31%	9%	33%
III	7%	2%	19%	15%	63%

5. Application

According to the research results, water-flooded zones in 315 reservoirs of 75 new wells in the study area from 2019 to 2021 were evaluated, and the coincidence rate (Table 6) of quantitative calculation of water production rate of water-flooded zones is as high as 91%. The interpretation results of some wells are inconsistent with the actual production data, which is believed to attribute to the fact that the error of oil column height is amplified in the zone close to the oil–water contact, so the calculation error of initial resistivity of oil zone is large to affect the calculation accuracy of water cut.

Table 6. Interpretation results of some new wells in the P Formation.

Well	Depth_T	Depth_B	Class of Reservoir	Regression Resistivity	Calculated Water Production Rate, %	Water-Flooding Level	Well Production Data
XX28	790.9	793.2	II	7.74	32.2	Moderately water-flooded	f_w = 62.9%
XX28	794.7	801.2	II	7.02	85.0	Highly water-flooded	
XX36	800.4	804.5	I	17.94	96.9	Highly water-flooded	f_w = 94.1%
XX36	804.5	806.6	I	18.07	99.5	Highly water-flooded	
XX36	811.0	812.7	I	17.21	92.5	Highly water-flooded	
XX36	810.7	814.0	II	12.31	99.5	Highly water-flooded	
XX46	816.3	817.6	II	6.08	12.2	Weakly water-flooded	f_w = 57.6%
XX46	818.9	824.4	I	9.15	64.0	Moderately water-flooded	
XX46	826.0	826.6	II	9.29	75.5	Moderately water-flooded	
XX46	829.6	838.9	I	12.83	99.2	Highly water-flooded	
XX46	840.5	841.0	II	4.42	67.8	Moderately water-flooded	
XX46	842.0	842.8	III	2.50	−55.3	Non-water-flooded	
XX37	787.2	790.7	II	8.28	89.05	Highly water-flooded	f_w = 79.6%
XX37	791.9	794.4	I	8.05	73.59	Moderately water-flooded	

6. Conclusions

The resistivity is directly related to the water saturation, and the oil column height is the reflection of the capillary pressure. The J-functions of grouped capillary pressure curves are applied to the resistivity vs. oil column height crossplot to realize the classification of reservoirs with an unclear porosity–permeability relationship. Oil column height and GR are the key controls on the initial resistivity of the reservoirs in the study area. The initial resistivity can be reconstructed by using the multiple regression method. The relative permeability test is performed for the reservoirs. For each class of reservoirs, the relationship between water cut and resistivity decline rate is established, and the water-flooding intensity is finely divided. This method can help improve the accuracy of the quantitative evaluation of water-flooded zones.

Field application reveals that the classification of sandstone reservoirs with a complex porosity–permeability relationship and quantitative evaluation of water-flooded zones contribute a coincidence rate of more than 90%, which meets the required interpretation accuracy of water-flooded zones in oilfields. However, this method yields a relatively low accuracy in evaluating the water-flooded zones close to the oil–water contact.

Author Contributions: Conceptualization and methodology, D.Z. and Y.L. (Yuming Liu); investigation, J.N. and A.Z.; data curation, Y.L. (Yaping Lin) and L.Z.; writing—original draft preparation, J.W.; writing—review and editing, X.L. All authors have read and agreed to the published version of the manuscript.

Funding: This work is supported by the Major scientific and technological projects of PetroChina (2021DJ3201).

Institutional Review Board Statement: Not applicable.

Informed Consent Statement: Not applicable.

Data Availability Statement: Not applicable.

Conflicts of Interest: The authors declare no conflict of interest.

References

1. Sagyndikov, M.; Mukhambetov, B.; Orynbasar, Y.; Nurbulatov, A.; Aidarbayev, S. Evaluation of polymer flooding efficiency at brownfield development stage of giant Kalamkas oilfield, western Kazakhstan. In Proceedings of the SPE Annual Caspian Technical Conference and Exhibition, Astana, Kazakhstan, 31 October–2 November 2018.
2. Muratov, I.M. Structure of the oil and gas Pools of the Jurassic Horizons of the Kalamkas field. *Petrol. Geol. A Dig. Russ. Lit. Pet. Geol.* **1984**, *21*, e511–e512.
3. Li, X.; Jin, R.; Fu, L.; Xu, B.; Zhang, Z. Water-Out Characteristics and Remaining Oil Distribution of Delta Front Reservoir—Take J-2C Reservoir of Kalamkas Oilfield in Kazakhstan as an Example. In Proceedings of the International Field Exploration and Development Conference 2018, Xi'an, China, 18–20 September 2018; Springer: Singapore, 2018; pp. 1527–1535.
4. Ni, J.; Zhao, D.; Liao, X.; Li, X.; Fu, L.; Chen, R.; Xia, Z.; Liu, Y. Sedimentary Architecture Analysis of Deltaic Sand Bodies Using Sequence Stratigraphy and Seismic Sedimentology: A Case Study of Jurassic Deposits in Zhetybay Oilfield, Mangeshrak Basin, Kazakhstan. *Energies* **2022**, *15*, 5306. [CrossRef]
5. Lin, Q. Technology and Practice of stabilizing oil production and controlling water cut in Kalamkas Oilfield in central Asia. *China Oil Gas J.* **2015**, *22*, e48–e54.
6. Tangparitkul, S.; Saul, A.; Leelasukseree, C.; Yusuf, M.; Kalantariasl, A. Fines migration and permeability decline during reservoir depletion coupled with clay swelling due to low-salinity water injection: An analytical study. *J. Pet. Sci. Eng.* **2020**, *194*, 107448. [CrossRef]
7. Wang, X.; Zhang, F.; Li, S.; Dou, L.; Liu, Y.; Ren, X.; Chen, D.; Zhao, W. The Architectural Surfaces Characteristics of Sandy Braided River Reservoirs, Case Study in Gudong Oil Field, China. *Geofluids* **2021**, *2021*, 8821711. [CrossRef]
8. Xu, L.; Zhang, J.; Ding, J.; Liu, T.; Shi, G.; Li, X.; Dang, W.; Cheng, Y.; Guo, R. Evaluation and optimization of flow unit division methods. *Lithol. Reserv.* **2015**, *27*, 74–80.
9. Hearn, C.L.; Ebanks, W., Jr.; Tye, R.S. Geological factors in influencing reservoir performance of the Hartzog Draw Field, Wyoming. *Petrol. Tech.* **1984**, *36*, 1335–1344. [CrossRef]
10. Yang, J.; Fan, T.; Ma, H. On Log Interpretation of water flooded layer with reservoir classification method. *Well Logging Technol.* **2010**, *34*, 238–241.
11. Hui, G.; Wang, Y.; Yan, L.; Li, J.; Liu, L. Method for water-flooded layer evaluation in extra-low permeability reservoir in WY block of AS oilfield flooded by fresh-water. *J. Southwest Pet. Univ. (Sci. Technol. Ed.)* **2016**, *38*, 138.
12. Wang, Z.; He, G. The classification method and application of reservoir flow units. *Nat. Gas Geosci.* **2010**, *21*, 362–366.
13. Gunter, G.W.; Finneran, J.M.; Hartmann, D.J.; Miller, J.D. Early determination of reservoir flow units using an integrated petrophysical method. In Proceedings of the SPE Annual Technical Conference and Exhibition, San Antonio, TX, USA, 5–8 October 1997.
14. Wang, S.; Wu, S.; Cai, F.; Li, Y.N.; Chen, Y.X. Sedimentary Facies of Kumkol Formation of Upper Jurassic in Kumkol Oilfield, South Turgay Basin. *Xi'an Shiyou Univ. (Nat. Sci. Ed.)* **2012**, *27*, 15–20.
15. Chen, C.; Song, X.; Li, J. Dominant flow channels of point-bar reservoirs and their control on the distribution of remaining oils. *Acta Pet. Sin.* **2012**, *33*, 257–263.
16. Huang, H.; Li, R.; Xiong, F.; Hu, H.; Sun, W.; Jiang, Z.; Chen, L.; Wu, L. A method to probe the pore-throat structure of tight reservoirs based on low-field NMR: Insights from a cylindrical pore model. *Mar. Pet. Geol.* **2020**, *117*, 104344. [CrossRef]
17. Pirrone, M.; Battigelli, A.; Ruvo, L. Lithofacies Classification of Thin Layered Reservoirs Through the Integration of Core Data and Dielectric Dispersion Log Measurements. In Proceedings of the SPE Annual Technical Conference and Exhibition, Amsterdam, The Netherlands, 27–29 October 2014.
18. Al-Mudhafar, W.J. Integrating machine learning and data analytics for geostatistical characterization of clastic reservoirs. *J. Pet. Sci. Eng.* **2020**, *195*, 107837. [CrossRef]

19. Lee, S.H.; Datta-Gupta, A. Electrofacies characterization and permeability predictions in carbonate reservoirs: Role of multivariate analysis and nonparametric regression. In Proceedings of the SPE Annual Technical Conference and Exhibition, Houston, TX, USA, 3–6 October 1999.
20. Ameur-Zaimeche, O.; Zeddouri, A.; Heddam, S.; Kechiched, R. Lithofacies prediction in non-cored wells from the Sif Fatima oil field (Berkine basin, southern Algeria): A comparative study of multilayer perceptron neural network and cluster analysis-based approaches. *J. Afr. Earth Sci.* **2020**, *166*, 103826. [CrossRef]
21. Bressan, T.S.; de Souza, M.K.; Girelli, T.J.; Junior, F.C. Evaluation of machine learning methods for lithology classification using geophysical data. *Comput. Geosci.* **2020**, *139*, 104475. [CrossRef]
22. Tang, H.; White, C.; Zeng, X.; Gani, M.; Bhattacharya, J. Comparison of multivariate statistical algorithms for wireline log facies classification. *AAPG Annu. Meet. Abstr.* **2004**, *88*, 13.
23. Ren, X.; Hou, J.; Song, S.; Liu, Y.; Chen, D.; Wang, X.; Dou, L. Lithology identification using well logs: A method by integrating artificial neural networks and sedimentary patterns. *J. Pet. Sci. Eng.* **2019**, *182*, 106336. [CrossRef]
24. Utepov, M.S.; Sarbopeyev, O.K. Improvement of the efficiency of repair and insulation works to limit water product from reservoir, using new technologies in Kalamkas oilfield. *Kazakhstan J. Oil Gas Ind.* **2020**, *2*, 70–78. [CrossRef]
25. Sagyndikov, M.; Satbayev University; Salimgarayev, I.; Ogay, E.; Seright, R.; Kudaibergenov, S. Assessing polyacrylamide solution chemical stability during a polymer flood in the Kalamkas field, Western Kazakhstan. *Bull. Karaganda Univ. Chem. Ser.* **2022**, *105*, 99–112. [CrossRef]
26. Nguyen, C.; Loi, G.; Russell, T.; Shafian, S.M.; Zulkifli, N.; Chee, S.; Razali, N.; Zeinijahromi, A.; Bedrikovetsky, P. Well inflow performance under fines migration during water-cut increase. *Fuel* **2022**, *327*, 124887. [CrossRef]
27. Bedrikovetsky, P.; de Siqueira, F.D.; Furtado, C.A.; Souza, A.L.S. Modified particle detachment model for colloidal transport in porous media. *Transp. Porous Media* **2011**, *86*, 353–383. [CrossRef]
28. Tian, Z.; Mu, L.; Sun, D.; Lv, L.H. Logging attributes and mechanism study of grit water-flooding reservoir. *Acta Pet. Sin.* **2002**, *23*, 50–55.
29. Liu, Y.; Hou, J.; Wang, L.; Xue, J.; Liu, X.; Fu, X. Architecture analysis of braided river reservoir. *J. China Univ. Pet. Ed. Nat. Sci.* **2009**, *30*, 7–11.
30. Zhao, W. Experiment research on the rock resistivity properties of watered-out formation. *Oil Gas Recovery Technol.* **1995**, *2*, 32–39.
31. National Energy Administration. *Specification for Logging Data Processing and Interpreting of Water-Flooded Zone: SY/T 6178-2017[S]*; Petroleum Industry Press: Beijing, China, 2017.
32. Li, C.; Zhu, S. Some topics about water cut rising rule in reservoirs. *Lithol. Reserv.* **2016**, *28*, 1–5.
33. Archie, G.E. The electrical resistivity log as an aid in determining some reservoir characteristics. *Pet. Trans. Aime* **1942**, *146*, 54–61. [CrossRef]
34. Tan, F.; Li, H.; Xu, C.; Li, Q.; Peng, S. Quantitative evaluation methods for water-flooded layers of conglomerate reservoir based on well logging data. *Pet. Sci.* **2010**, *7*, 485–493. [CrossRef]
35. Lin, Y.; Guo, Z.; Sheng, S.; Zheng, J.; Luo, M.; Liang, H. A New Method for Flooded Layer Evaluation by Logging with Strong Heterogeneous in Heavy Oil Reservoirs, K Field, Central Asia. In Proceedings of the International Field Exploration and Development Conference 2018, Xi'an, China, 18–20 September 2018; Springer: Singapore, 2018; pp. 328–339.